

# QUALIFICATION STUDIES ON THE FINITE ELEMENT CODE HONDO II AGAINST SOME BENCHMARK ANALYTICAL PROBLEMS

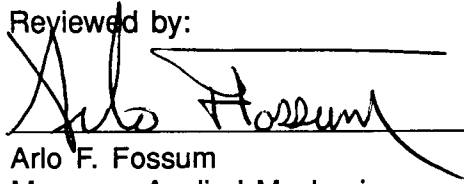
Prepared for  
**Nuclear Regulatory Commission**  
**Contract NRC-02-88-005**

Prepared by  
**T. Brandshaug**  
**B. Dasgupta**  
**B. H. G. Brady**  
**S. M. Hsiung**  
**A. H. Chowdhury**

**Center for Nuclear Waste Regulatory Analyses**  
**San Antonio, Texas**

**February 1990**

Reviewed by:



Arlo F. Fossum  
Manager, Applied Mechanics  
Southwest Research Institute

Approved by:



Allen R. Whiting, Director  
Waste Systems Engineering & Integration



Wesley C. Patrick  
Technical Director



Bruce Mabrito, Director  
Quality Assurance

# QUALIFICATION STUDIES ON THE FINITE ELEMENT CODE HONDO II AGAINST SOME BENCHMARK ANALYTICAL PROBLEMS

## TABLE OF CONTENTS

	Page
PURPOSE .....	1
SCOPE .....	1
1. INTRODUCTION .....	1
1.1 BACKGROUND .....	1
1.2 GENERAL FEATURES OF HONDO II .....	2
2. CYCLIC LOADING OF A SPECIMEN WITH A SLIPPING JOINT .....	2
2.1 PROBLEM DEFINITION .....	2
2.2 PURPOSE .....	2
2.3 PROBLEM SPECIFICATION .....	2
2.4 ASSUMPTIONS .....	6
2.5 CONCEPTUAL MODEL .....	6
2.6 COMPUTER MODEL .....	8
2.7 RESULTS AND DISCUSSION .....	10
3. SLIP IN A JOINTED BODY INDUCED BY A HARMONIC SHEAR WAVE .....	13
3.1 PROBLEM STATEMENT .....	13
3.2 PURPOSE .....	13
3.3 ANALYTICAL SOLUTION .....	13
3.4 ANALYSIS WITH HONDO II .....	16
3.5 RESULTS .....	20
4. CODE LIMITATIONS .....	22
5. SUMMARY AND CONCLUSIONS .....	27
6. REFERENCES .....	28
APPENDIX 1 – HONDO II INPUT DATA FILES .....	29

## LIST OF FIGURES

		Page
2.1	Specimen with Embedded Joint .....	4
2.2	Stress-Displacement Relation for Elastic Specimen with Embedded Joint Subjected to Uniaxial Load Cycle [after Olsson, 1982] .....	5
2.3	Conceptual Model of Elastic Specimen Containing Embedded Crack .....	7
2.4	Discretization of Elastic Medium into Four-Noded Quadrilateral Finite Elements .....	9
2.5	Axial Stress vs Axial Displacement During Loading and Unloading Using HONDO II (joint length = 0.47 m; friction coefficient = 0.287) .....	11
2.6	Axial Stress vs Axial Displacement During Loading and Unloading Predicted Using HONDO II (joint length = 0.71 m; friction coefficient = 0.287) .....	12
3.1	Problem Definition for Wave Propagation in a Jointed Continuum .....	14
3.2	Problem Geometry for Analysis of Slip Induced by a Harmonic Shear Wave .....	17
3.3	Finite Element Discretizations for Element Distributions (a) and (b) .....	18
3.4	History of Shear Stress at Points A through F for Solid Block and Discretization Scheme (a) .....	21
3.5	Shear Stress Histories for the Jointed Block at Points A through F, Coefficient of Friction = 0, Discretization Scheme (a) .....	23
3.6	Shear Stress Histories a Points A through F, Coefficient of Friction = 0, Discretization Scheme (b) .....	24
3.7	Shear Stress Histories at Points A through F, Coefficient of Friction = 0.286, Discretization Scheme (b) .....	25
3.8	Shear Stress Histories at Points A through F, Coefficient of Friction = 0.7, Discretization Scheme (b) .....	26

## LIST OF TABLES

	Page
2.1 Hondo Input Parameters .....	8
2.2 Comparison of HONDO II Results with Conceptual Model Solution for Cyclic Loading of a Specimen with a Slipping Crack .....	10
3.1 Mechanical Properties of the Elastic Media and Discontinuity .....	19

# QUALIFICATION STUDIES ON THE FINITE ELEMENT CODE HONDO II AGAINST SOME BENCHMARK ANALYTICAL PROBLEMS

## PURPOSE

The purpose of this report is to present the results of studies that assess the performance of the two-dimensional finite element code, HONDO II, in analysis of some benchmark problems in the mechanics of discontinuous rock.

## SCOPE

Qualification studies on a computer code involve assessment of code performance by comparison of computed solutions for particular problems with the analytical solutions to these problems, or suitable approximations to the analytical solutions. In the current study, the original intention was to consider four benchmark problems, two quasi-static and two dynamic, examining the performance of the joint model in HONDO II, which is a Coulomb formulation based on velocity-dependent friction. However, because limitations of the code were observed, specifically the inability of the joint model to reproduce the essential feature of hysteretic response, the scope of the work was restricted to one quasi-static and one dynamic problem.

## 1. INTRODUCTION

### 1.1 BACKGROUND

This report is the second of a series of reports to be prepared on qualification studies of the performance of computer codes, which may simulate the behavior of discontinuous rock masses. Implicitly, it includes an assessment of formulations of joint deformation, which are incorporated in the codes. The justification for and scope of this work is outlined in Task 3, Assessment of Analytical Models/Computer Codes, Seismic Rock Mechanics Project (Hsiung et al., 1989). The purpose of the comparative studies on code performance is to determine which of the codes identified in an earlier effort (Kana et al., 1989) are appropriate and efficient simulators of the behavior of jointed rock masses under repeated dynamic loading. The studies are of two types, which together are intended to evaluate the constitutive relations for rock masses and discontinuities and their implementation in various codes for seismic analysis of excavations in jointed rock. The first type of study is intended to confirm that a code can reproduce the response of several well-established conceptual models of the performance of a jointed rock mass. In the second type of study, each qualified code from the first study will be used to analyze the dynamic response of well-designed and executed laboratory experiments to be performed in Task 2 (Hsiung et al., 1989) on elements of jointed rock. At the conclusion of these studies, it will be established which codes satisfactorily represent the fundamental dynamics of jointed rock, and also can predict the behavior of a representative element of a jointed rock mass to an acceptable engineering tolerance.

In the earlier study (Kana et al., 1989), several codes, which may be applicable to the analysis of dynamic loading of excavations in a jointed, brittle, partially saturated, welded tuff rock mass, were identified as current candidates for assessment. The identified codes include the distinct element codes UDEC and 3DEC (Cundall, 1988), the discrete element code DECICE (Williams et al., 1985), the finite element codes HONDO II and SPECTROM-331 (Key, 1986), and the boundary element code BEST3D (Banerjee and Ahmad, 1985). These codes may model the dynamic performance of jointed rock masses. The particular feature of each code, which qualifies it for consideration in the comparative studies, is the formulation of an

interface on which rigid body slip or separation can occur under static or dynamic loading. Whether the interface meets the requirements for satisfactory simulation of discontinuous deformation of jointed rock is the concern of these studies.

The two benchmark problems employed in the current qualification studies on HONDO II represent the simplest quasi-static and dynamic analyses of the loading and performance of jointed rock. A jointed block subject to cyclic loading (Olsson, 1982; Brady et al., 1985) is the only static problem for which an exact solution is available. For dynamic analysis, the solution for the transmission of a harmonic incident shear wave across a cohesive interface in a bar (Miller, 1978) is also exact. In both these problems, the joint is assumed to be rigid-plastic in shear, with the limiting shear resistance determined by simple Coulomb friction.

The joint deformation model implemented in HONDO II assumes rigid-plastic deformation under shear loading, with the limiting shear strength defined by Coulomb friction. As will be noted later, the formulation is complicated by the inclusion of terms that account for dynamic friction and decay of dynamic friction with decreasing velocity. In principle, however, the joint model in the code is compatible with that employed in the benchmark problems. On that basis, the comparison between the numerical solution to a problem and the analytical solution should be rigorous.

Details of the formulation of the HONDO II code have been documented by Key et al. (1978). Although there have been some enhancements to the code since preparation of that documentation, it is understood that these do not affect its capacity to analyze the benchmark problems considered here. The general features of the code are as follows.

## 1.2 GENERAL FEATURES OF HONDO II

HONDO II is a finite element-based computer code for the analysis of large deformation, elastic and inelastic transient dynamic response of solids, for which a plane strain or axisymmetric representation is appropriate. The Galerkin formulation of the finite element method is used to generate the spatial discretization (Zienkiewicz, 1977). Four-noded rectangular elements are used, and the motion is assumed to vary bi-linearly over the element using isoparametric coordinates. The code provides the option to use a one-point or two-point Gaussian quadrature, allowing stresses to be evaluated either at one or four integration points within the element, respectively.

The resulting simultaneous equations in time are integrated using an explicit central difference expression for velocity and acceleration. Because this integration procedure is conditionally stable with respect to the timestep size, the code continually monitors the step size during the calculations, and updates the size of the time step if necessary. In the course of the calculation sequence, a global quality assessment of the calculations is made by continuously comparing the energy supplied to the system with the sum of the kinetic energy and the internal energy of the system.

In terms of capacity to simulate material constitutive behavior, the code offers a choice of several material models such as elastic, elastic-plastic including strain hardening, crushable foam or soil behavior, and viscoelastic behavior. The code is written such that new material subroutines can be added easily.

A sliding interface is simulated in the code. As noted above, the constitutive behavior of the interface for shear deformation is characterized as rigid-perfectly plastic. Initiation of sliding is governed by a Coulomb friction model. The shear force acting parallel to the interface is given by the expression

$$G = [\mu_{\infty} + (\mu_0 - \mu_{\infty})e^{-\gamma v}]F_n \quad (1.1)$$

In this expression,  $\mu_0$  and  $\mu_\infty$  are friction coefficients for low and high sliding velocities, respectively, while  $\gamma$  is a decay constant characteristic of the transition between low and high sliding velocities.  $F_n$  is the normal force acting across the interface.

In specifying initial and boundary conditions, only velocities may be prescribed. The boundary conditions available are: (1) kinematic boundaries where nodal points are prevented from displacing in either the vertical or horizontal direction, or both, and (2) pressure boundaries, where a uniform or linearly varying pressure can be prescribed along an element side as a function of time.

Although HONDO II permits time-dependent pressure boundaries, the same history function is applied to all boundary pressures. However, the arrival time of the pressure can be different for different boundaries. The code permits specification of a rigid boundary where a stiffness can be prescribed.

## 2. CYCLIC LOADING OF A SPECIMEN WITH A SLIPPING JOINT

### 2.1 PROBLEM DEFINITION

This problem concerns an elastic block with an inclined internal closed joint (Figure 2.1) subject to a cycle of uniaxial loading.

A linearly-increasing force  $F$  is applied to one end of the block, and the other end is fixed. Upon loading, inelastic slip takes place along the joint. At some point, the applied force is decreased linearly until zero force remains. Olsson (1982) showed that the stress-displacement relation for the loaded specimen is composed of three distinct components (Figure 2.2):

- (1) a loading segment (OA) which involves elastic deformation and slip along the joint;
- (2) an initial unloading segment (AB), where the joint does not slip; and
- (3) a final unloading segment (BO), again with elastic deformation and slip.

### 2.2 PURPOSE

The purpose of this problem is to evaluate the simulation of discontinuous rock deformation, and to test the formulation of the relations in HONDO II representing joint deformation (Key et al., 1978). Other code functions tested by this problem include:

- (1) the ability of the code to model solid elastic behavior; and
- (2) the ability of the code to model quasi-static behavior.

### 2.3 PROBLEM SPECIFICATION

A single inclined joint is located in an elastic block. The mechanical properties of the medium and dimensions of the block are listed below.

Young's modulus ( $E'$ )	88.9 GPa
Poisson's ratio ( $\nu'$ )	0.26
height (H)	2 m
width (W)	1 m

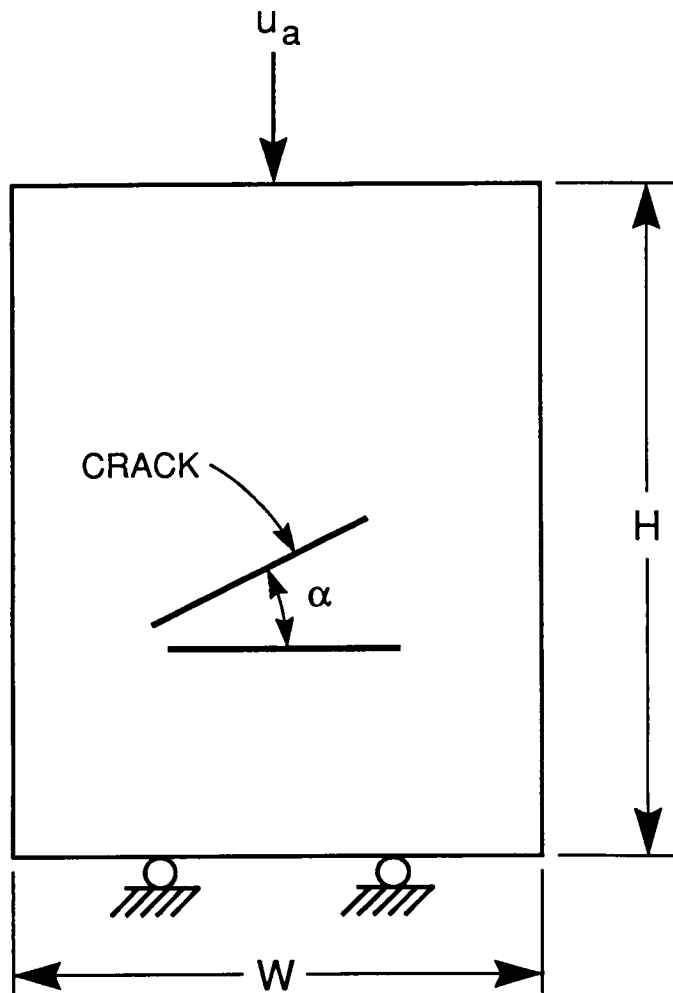


Figure 2.1 Specimen with Embedded Crack



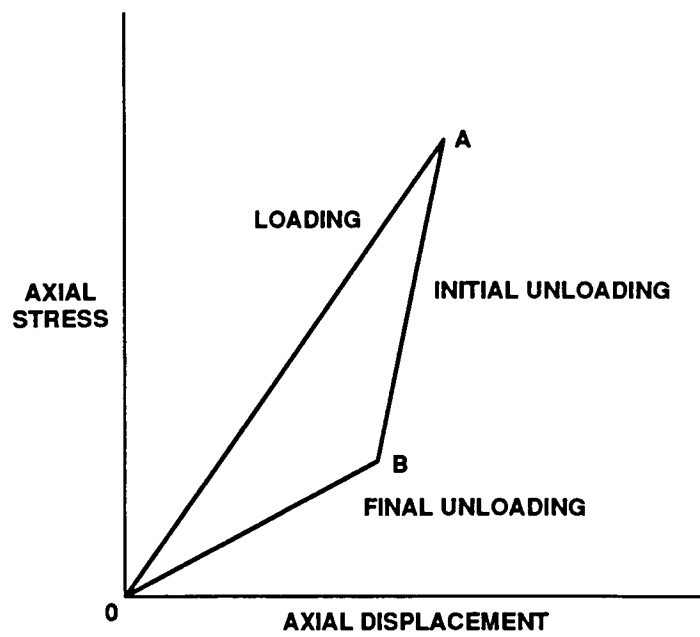


Figure 2.2 Stress-Displacement Relation for Elastic Specimen with Embedded Joint Subjected to Uniaxial Load Cycle [after Olsson, 1982]

The mechanical and geometric properties of the joint are as follows.

joint normal stiffness ( $K_n$ )	220 GPa/m
joint shear stiffness ( $K_s$ )	220 GPa/m
joint friction angle ( $\phi$ )	16°
joint inclination ( $\alpha$ )	45°
slipping segment of joint (l)	0.47 m <sup>(1)</sup>

<sup>(1)</sup>A slipping segment of 0.71 m was also investigated.

## 2.4 ASSUMPTIONS

The material in which the joint is embedded is linearly elastic, homogeneous, and isotropic. It is assumed in this analysis that the specimen is restrained perpendicular to the plane of analysis (i.e., plane strain conditions apply). It is further assumed that the joint can be represented by a single, finite length discontinuity (i.e., the material is continuous on either side of the discontinuity).

## 2.5 CONCEPTUAL MODEL

Several investigators have proposed simple conceptual models of a single, closed joint to explain phenomena associated with the deformational response of jointed rock (e.g., Walsh, 1965, and Jaeger and Cook, 1976). One such model is a single joint embedded in an elastic solid subjected to a cycle of uniaxial compression.

Brady et al. (1985) present relations for the three slopes in Figure 2.2 in terms of the elastic stiffness of the solid, the elastic and frictional properties of the joint, and the orientation of the joint. The conceptual model is illustrated in Figure 2.3. Note that the joint simulated in HONDO II, as in the simple conceptual model, is not continuous, but occupies only the distance identified by "1" in Figure 2.3.

In the conceptual model,  $k$  is the equivalent axial elastic stiffness of the block, including the through-going discontinuity. The equivalent elastic compliance is given by

$$\frac{1}{k} = \frac{H}{WE'} + \frac{\cos^2\alpha}{K_n L} + \frac{\sin^2\alpha}{K_s L} \quad (2.1)$$

where  $L = W/\cos\alpha$ .

It should be noted that the term  $(H/WE')$  in Eq. (2.1) represents the compliance of the solid in the conceptual model for plane stress conditions. The analysis in HONDO II is based on plane strain conditions. However, the plane strain solution can be determined from the plane stress solution with the following substitutions:

$$E = \frac{1 + 2\nu'}{(1 + \nu')^2} E' \quad (2.2)$$

$$\nu = \frac{\nu'}{1 + \nu'} \quad (2.3)$$

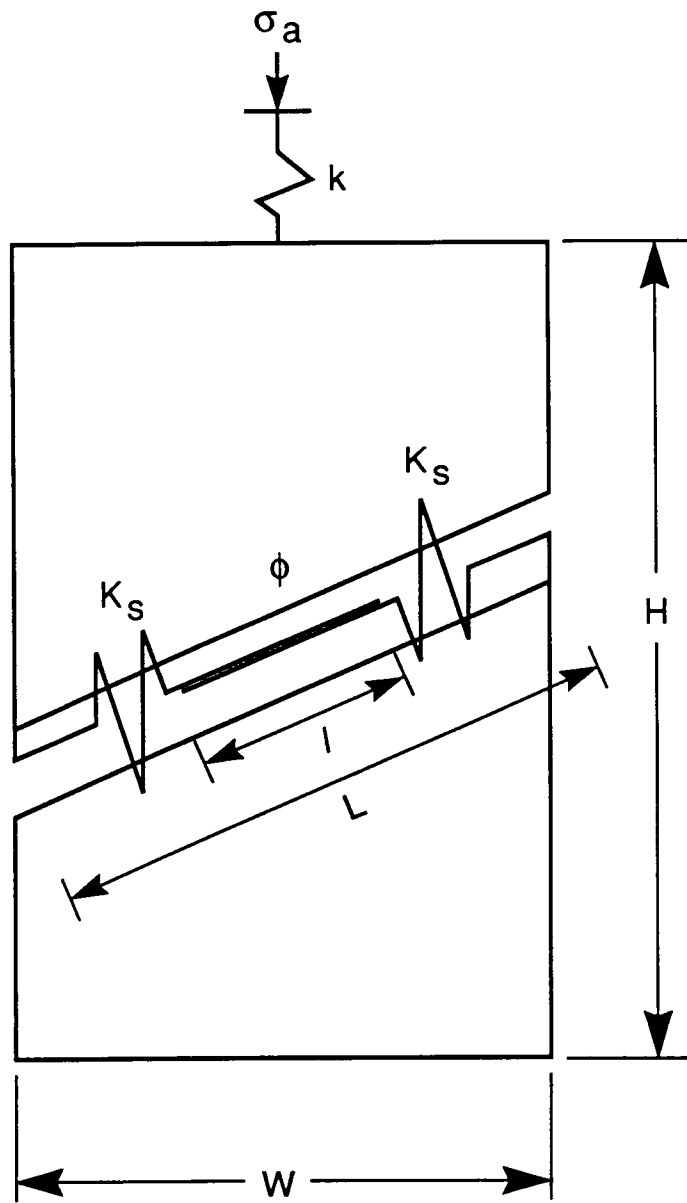


Figure 2.3 Conceptual Model of Elastic Specimen Containing Embedded Crack (After Brady et al., 1985)

where  $E'$  and  $\nu'$  are the Young's modulus and the Poisson's ratio of the medium, and  $E$  and  $\nu$  are the equivalent plane strain parameters.

The stiffnesses for the three slopes are therefore given as

$$\text{slope OA} = \frac{k}{1 + \frac{k \sin\alpha \sin(\alpha - \phi)}{K_s (L - 1) \cos\phi}} \quad (2.4)$$

$$\text{slope AB} = k \quad (2.5)$$

$$\text{slope BO} = \frac{k}{1 + \frac{k \sin\alpha \sin(\alpha + \phi)}{K_s (L - 1) \cos\phi}} \quad (2.6)$$

## 2.6 COMPUTER MODEL

In the HONDO II analysis, the elastic material is discretized into four-noded quadrilateral finite elements, as shown in Figure 2.4.

As noted in Section 1.2, the constitutive relation for the sliding interface in HONDO II is characterized as rigid-perfectly plastic. Initiation of sliding is governed by a Coulomb friction relation between shear and normal forces operating on the interface. The shear force defined in Eq. (1.1) includes friction coefficients  $\mu_0$  and  $\mu_\infty$  for low and high sliding velocities, respectively, and a decay constant  $\gamma$  characteristic of the transition between the low and high sliding velocities.  $F_n$  is the normal force across the interface. In the current analysis,  $\mu_\infty$  and  $\gamma$  were assigned values of zero. Two elastic moduli,  $E_1$  and  $E_2$ , are also required to describe the sliding interface. These moduli are associated with the determination of the normal contact forces at the interface. For the current problem, these moduli were assigned the same value as the Young's modulus of the solid material.

For the sake of completeness, the values of the input parameters used in HONDO II for this problem are listed in Table 2.1.

Table 2.1  
HONDO II Input Parameters

Rock Material	Sliding Interface
$E = 85.1 \text{ GPa}^{(1)}$	$\mu_0 = 0.287^{(2)}$
$\nu = 0.21^{(1)}$	$\mu_\infty = 0.$
$\rho = 2850 \text{ kg/m}^3$	$\gamma = 0.$
	$E_1 = 85.1 \text{ GPa}$
	$E_2 = 85.1 \text{ GPa}$

<sup>(1)</sup>Values reflect adjustment for use in plane strain calculations as compared to those listed in Section 2.3

<sup>(2)</sup>Other values used were 0. and 0.7.

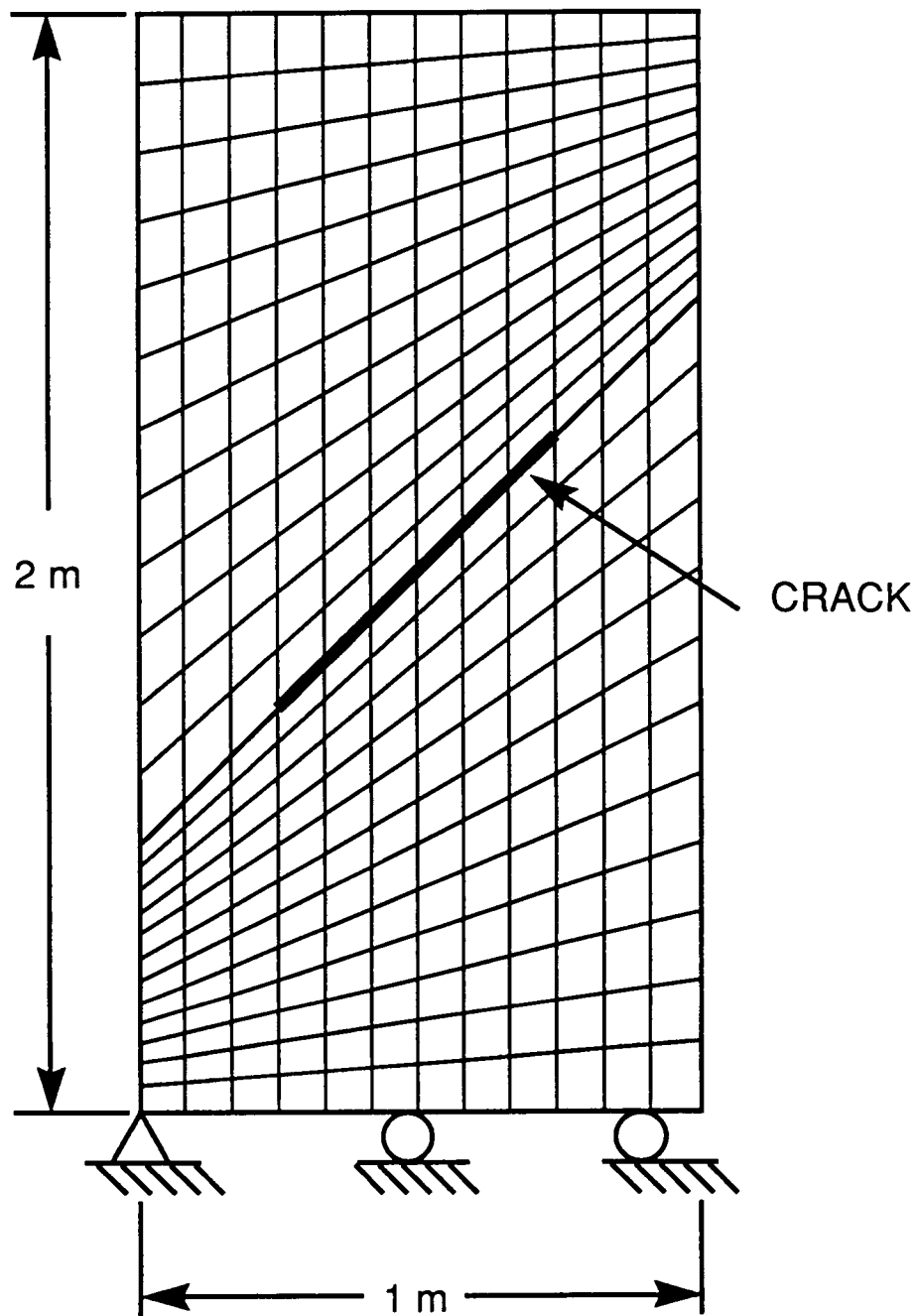


Figure 2.4 Discretization of Elastic Medium into Four-Noded Quadrilateral Finite Elements

## 2.7 RESULTS AND DISCUSSION

The model shown in Figure 2.1 was loaded from 0 to 8.5 MPa, and subsequently unloaded to 0. To represent quasi-static behavior, the load and unload phases were each performed over a 0.1 second time interval. The global axial stiffness was calculated every 0.005 second timestep as the ratio of the average vertical stress to the maximum vertical displacement. Figure 2.5 is a plot of the calculated vertical stress versus vertical displacement for the complete load/unload cycle for a friction coefficient,  $\mu_o$ , of 0.287. It is notable that the stress/displacement behavior indicated in this figure does not reproduce the characteristic hysteresis in the load cycle which was described previously for the conceptual model. Because the constitutive model of the sliding interface for shear is rigid-perfectly plastic, the global axial stiffness immediately upon unloading should reflect the elastic behavior of the intact material. That is, because the interface is frictionally locked at this stage, there should be no contribution from deformation of the interface to the overall specimen deformation. This behavior is not expressed in the results of the analysis shown in Fig. 2.5.

The amount of hysteresis in a load cycle depends on the coefficient of friction for the joint, with hysteresis non-existent for a frictionless joint and increasing with the magnitude of the coefficient. To examine the effect of this parameter in the current analysis, joint friction coefficients of 0 and 0.7 were also investigated. However, the results were identical to those for  $\mu_o$  of 0.287. As one would expect, increasing the length of the inclined joint from 0.47 m to 0.71 m results in a decrease in the predicted global stiffness, as indicated by a comparison of Figs. 2.5 and 2.6. Even at the higher value of the coefficient, no hysteresis was observed in the unloading phase of the cycle. Without investigating the details of the solution procedure in HONDO II, it is not possible to identify the reasons for its failure to reproduce hysteresis during a loading cycle.

A direct comparison of the calculated global axial stiffness with those determined from the conceptual model is presented in Table 2.2. Besides the discrepancy during unloading, the predicted stiffness during loading is slightly higher than that determined from the conceptual model. Thus, with the exception of not being able to reproduce the hysteretic behavior of the jointed block during unloading, HONDO II appears capable of modelling solid elastic behavior and quasi-static behavior.

Table 2.2  
Comparison of HONDO II Results with Conceptual Model Solution for  
Cyclic Loading of a Specimen with a Slipping Crack

Loading Segment	Conceptual Model Stiffness (GPa/m)	HONDO II Crack Length = 0.47 m Stiffness (GPa/m)	HONDO II Crack Length = 0.71 m Stiffness (GPa/m)
Load (OA)	36.34	40.35	37.63
Unload (AB)	38.89	40.35	37.63
Unload (BO)	34.52	40.35	37.63

The simulation of discontinuities may be important in the context of evaluating the mechanical behavior of a geologic nuclear waste repository subject to static and dynamic loading. Therefore, the limitation in the

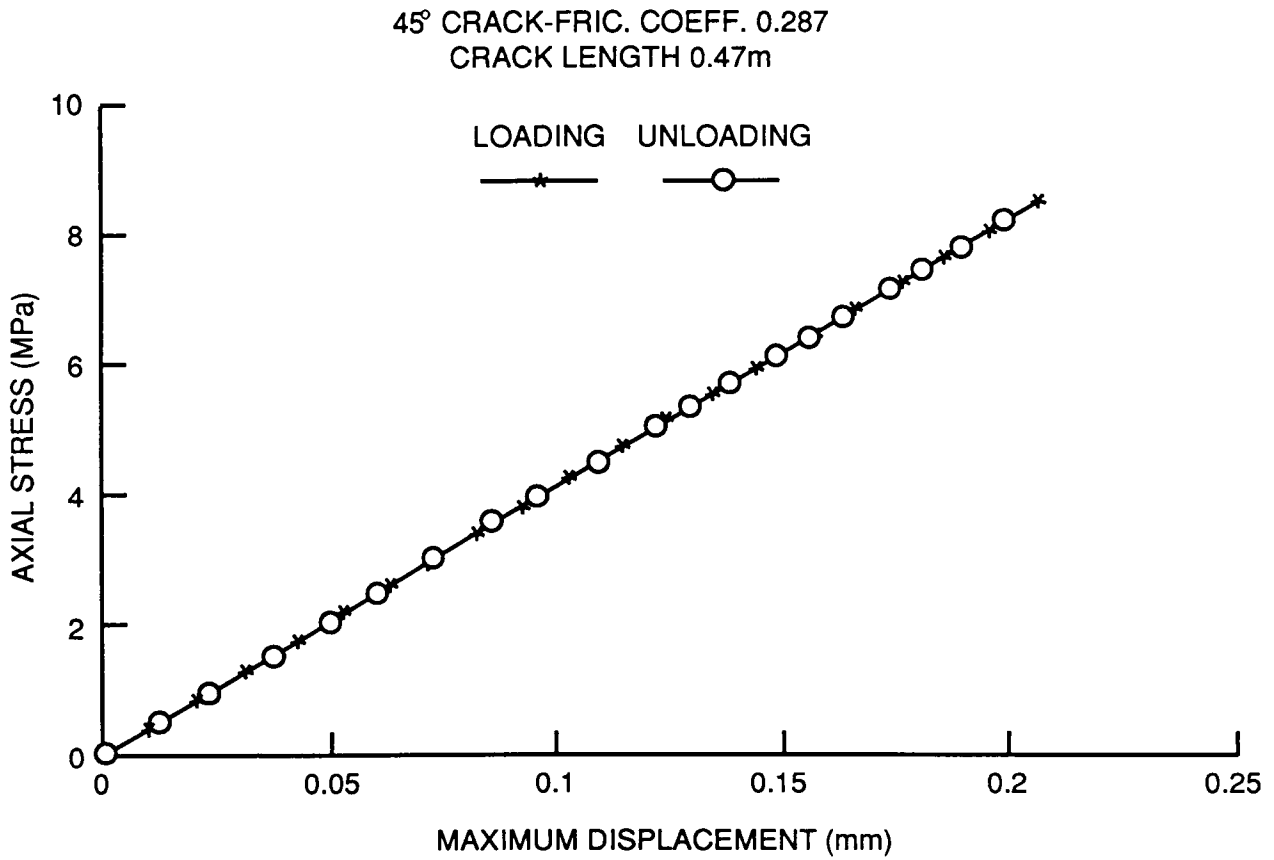


Figure 2.5 Axial Stress vs Axial Displacement During Loading and Unloading Using HONDO  
(joint length = 0.47 m; friction coefficient = 0.287)

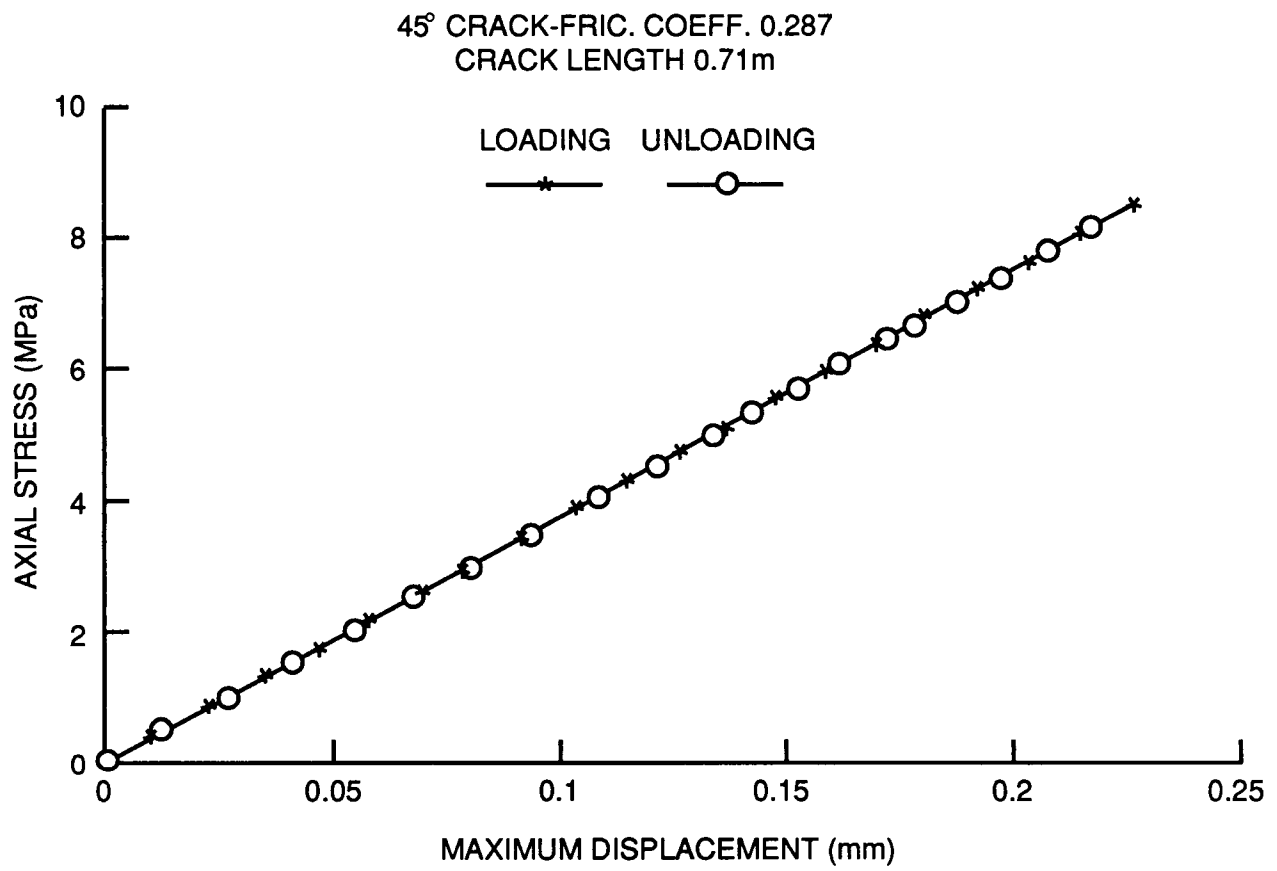


Figure 2.6 Axial Stress vs Axial Displacement During Loading and Unloading Predicted Using HONDO (joint length = 0.71 m; friction coefficient = 0.287)



capacity of HONDO II to simulate the details of deformation of jointed rock under pseudostatic cyclic loading imposes substantial restrictions on its usefulness for evaluating the performance of the host rock for a geologic repository under these loading conditions.

### 3. SLIP IN A JOINTED BODY INDUCED BY A HARMONIC SHEAR WAVE

#### 3.1 PROBLEM STATEMENT

This problem concerns the dynamic behavior of a plane discontinuity subjected to a propagating harmonic shear wave. The incident shear wave induces shear stress in the joint. When the shear stress exceeds the limiting shear strength, slip will occur, resulting in reflection, transmission and absorption of the strain energy in the shear wave. In an analysis reported by Miller (1978), closed-form solutions are established for the coefficients of reflection, transmission and absorption. The problem, shown in Figure 3.1, consists of two homogeneous, isotropic, semi-infinite, elastic bodies separated by a planar discontinuity and a normally-incident, plane harmonic shear wave. In principle, this problem can be modeled with HONDO II, because of assumed compatibility with the code formulation in terms of geometry, loading conditions and constitutive behavior of the interface between the elastic regions.

#### 3.2 PURPOSE

The purpose of this study is to evaluate the capacity of HONDO II to model the dynamic performance of a discontinuity in an elastic medium subject to loading by a harmonic shear wave. A comprehensive evaluation involves determination of the transmission, reflection and absorption coefficients from the numerical analysis and comparison with the closed-form solutions.

#### 3.3 ANALYTICAL SOLUTION

Miller (1987) solved the wave propagation problem considering dissimilar media, 1 and 2, on opposite sides of the interface. Referring to Figure 3.1, the incident wave is described by the expression

$$u_i = U \sin\left(\frac{\omega x}{C_i} - \omega t\right) \quad (3.1)$$

where  $C_i = \left(\frac{G_i}{\rho_i}\right)^{1/2}$  ( $i = 1,2$ ) represents the wave velocity in medium  $i$ ,

$U$  = amplitude, and

$\omega$  = frequency.

Miller showed that the shear displacement at the interface may be described by

$$d(t) = D \cos(\omega t - \phi) \quad (3.2)$$

where  $D$  = amplitude of joint shear, and

$\phi$  = phase shift occurring at the boundary.

The solution for  $D$  is obtained from the expression

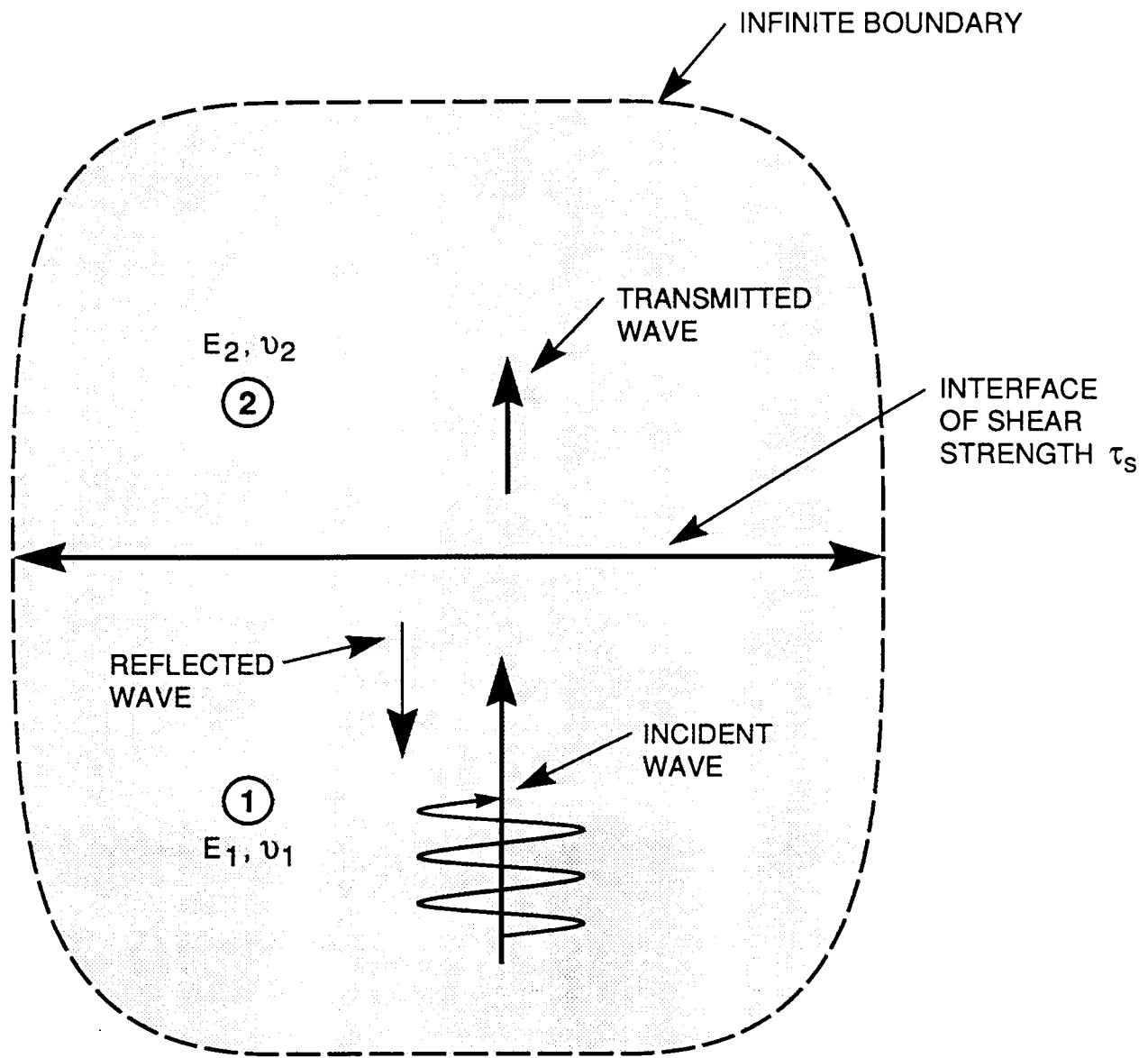


Figure 3.1 Problem Definition for Wave Propagation in a Jointed Continuum

$$C^2(D) + [\omega \gamma_1 \gamma_2 D / (\gamma_1 + \gamma_2) - S(D)]^2 = [2\omega U \gamma_1 \gamma_2 / (\gamma_1 + \gamma_2)^2] \quad (3.3)$$

where

$$C(D) = \frac{1}{\pi} \int_0^{2\pi} \tau_s (D \cos\theta, -\omega D \sin\theta) \cos\theta \, d\theta$$

$$S(D) = \frac{1}{\pi} \int_0^{2\pi} \tau_s (D \cos\theta, -\omega D \sin\theta) \sin\theta \, d\theta$$

$$\gamma_i = (\rho_i G_i)^{1/2}$$

If  $\tau_s$  is independent of displacement, as is assumed for a cohesive interface, considerable simplification of these expressions is possible.

After solving for D, the associated phase angle is given by

$$\phi = \tan^{-1} \left\{ [S(D) - \omega \gamma_1 \gamma_2 D / (\gamma_1 + \gamma_2)] / C(D) \right\} \quad (3.4)$$

Motion in the transmitted and reflected waves is defined by

$$u_T(x,t) = TU \sin \left( \frac{\omega x}{C_2} - \omega t + \phi_T \right) \quad (3.5)$$

$$u_R(x,t) = RU \sin \left( \frac{\omega x}{C_1} + \omega t + \phi_R \right)$$

where T and R are the transmission and reflection coefficients, and  $\phi_T$  and  $\phi_R$  (determined by  $\phi$ ) are phase shifts at the boundary.

By satisfying displacement conditions at the interface, it is found that

$$T = \left\{ \left[ \frac{D}{U} \sin\phi - 2 \right]^2 + \left[ \frac{D}{U^2} \cos^2\phi \right] \right\}^{1/2} \frac{\gamma_1}{\gamma_1 + \gamma_2} \quad (3.6)$$

$$R = \left\{ (D/U)^2 \cos^2\phi + [(D/U) \sin\phi + (\gamma_1 + \gamma_2) - 1]^2 \right\}^{1/2} \gamma_2 / (\gamma_1 + \gamma_2) \quad (3.7)$$

Equations 3.6 and 3.7 permit direct calculation of the transmission and reflection coefficients from the properties of the medium and the interface, and the wave characteristics.

An alternative interpretation of wave propagation coefficients T and R is in terms of the energy flux in the transmitted and reflected waves. If  $E_I$ ,  $E_R$  and  $E_T$  are the energy fluxes per unit area per cycle of oscillation for the incident, reflected and transmitted waves respectively, it may be shown that

$$T = \left( \gamma_1 / \gamma_2 \right)^{1/2} \left( E_T / E_I \right)^{1/2} \quad (3.8)$$

$$R = \left( E_R / E_I \right)^{1/2} \quad (3.9)$$

Further, energy is absorbed at the boundary by the dissipative nature of joint slip. An absorption coefficient is defined by

$$A = [1 - R^2 - (\gamma_2/\gamma_1) T^2]^{1/2} \quad (3.10)$$

In the assessment of HONDO II performance in modeling of joint slip, a technique is required to determine energy fluxes in the incident, transmitted and reflected waves. For the plane incident wave, the energy flux,  $E_I$ , per unit area and per unit cycle oscillation is given by (Kolsky, 1963)

$$E_I = \rho c \int_{t_1}^{t_1+T} v_I^2 dt \quad (3.11)$$

where  $v_I(t)$  = the particle velocity in the incident wave,

$T$  = period of ground motion

$$= 2\pi/\omega.$$

Similar expressions apply to fluxes in the transmitted and reflected waves. The various fluxes may be determined in a HONDO II analysis by numerical integration of the plots of  $v^2$  versus time. From these fluxes, Eqs. 3.8, 3.9 and 3.10 may be used to calculate the transmission, reflection and absorption coefficients. They may be compared with the coefficients calculated from the analytical solutions.

### 3.4 ANALYSIS WITH HONDO II

#### 3.4.1 Numerical Model

The problem geometry modeled with HONDO II is shown in Fig. 3.2. The block was modeled with an elastic solid of height  $h$  and width  $b$ , and was discretized into a set of four-noded quadrilateral finite elements. Two different distributions of elements were considered: (a) one element spanning the horizontal dimension of the block, and 161 in the vertical dimension; (b) three elements spanning the horizontal dimension, and 161 in the vertical dimension, as shown in Fig. 3.3. Because of a restriction in the code formulation preventing application of transverse boundary tractions, the harmonic shear wave was introduced to the system by applying a normal pressure on element 81 in the transverse direction. As shown in Figs. 3.3a and 3.3b, in each case the dynamic load was applied at the center of the model, so that there is no spurious reflection from the boundary AB. (Fig. 3.2) The time function of the normal pressure representing the transverse dynamic load is sinusoidal.

In setting boundary conditions for the analysis, displacements at boundaries AC, BD, AB and CD (Fig. 3.2) were restrained in the  $y$ -direction and unrestrained in the  $x$ -direction, to simulate plane shear wave conditions. The sliding interface was located between elements 121 and 122 (Fig. 3.2), at a distance "a" from the  $x$ -axis.

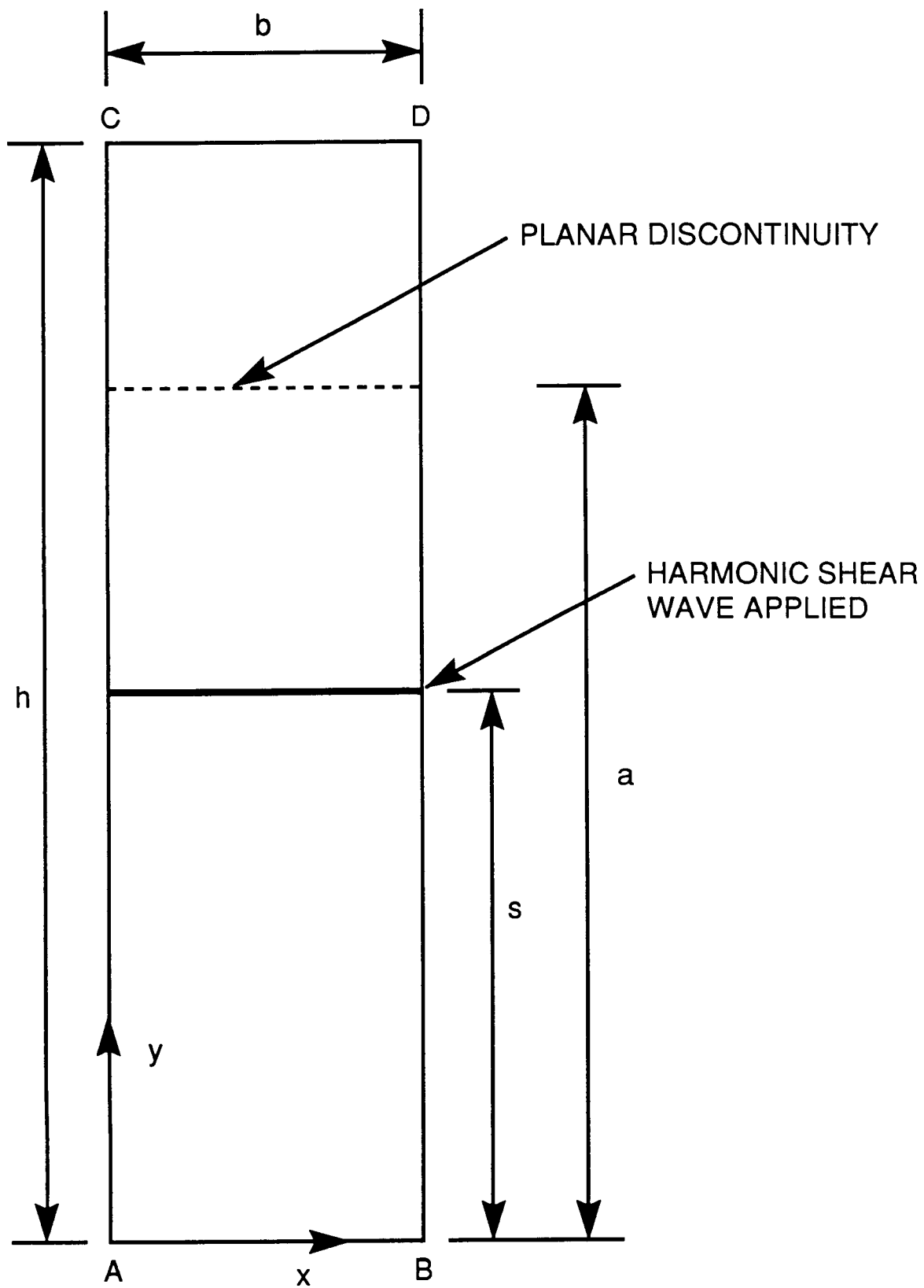
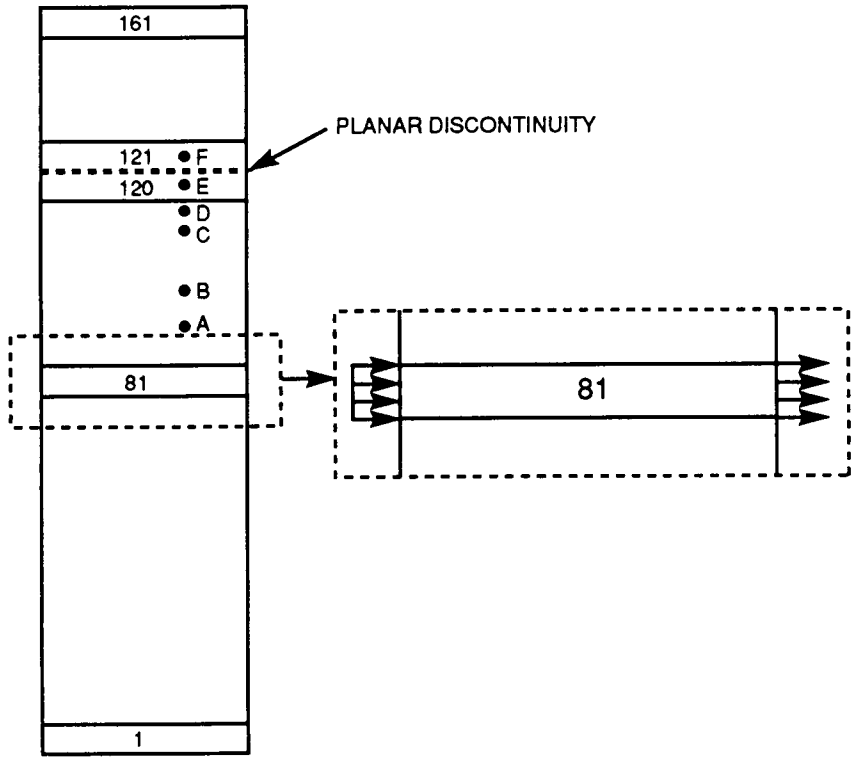
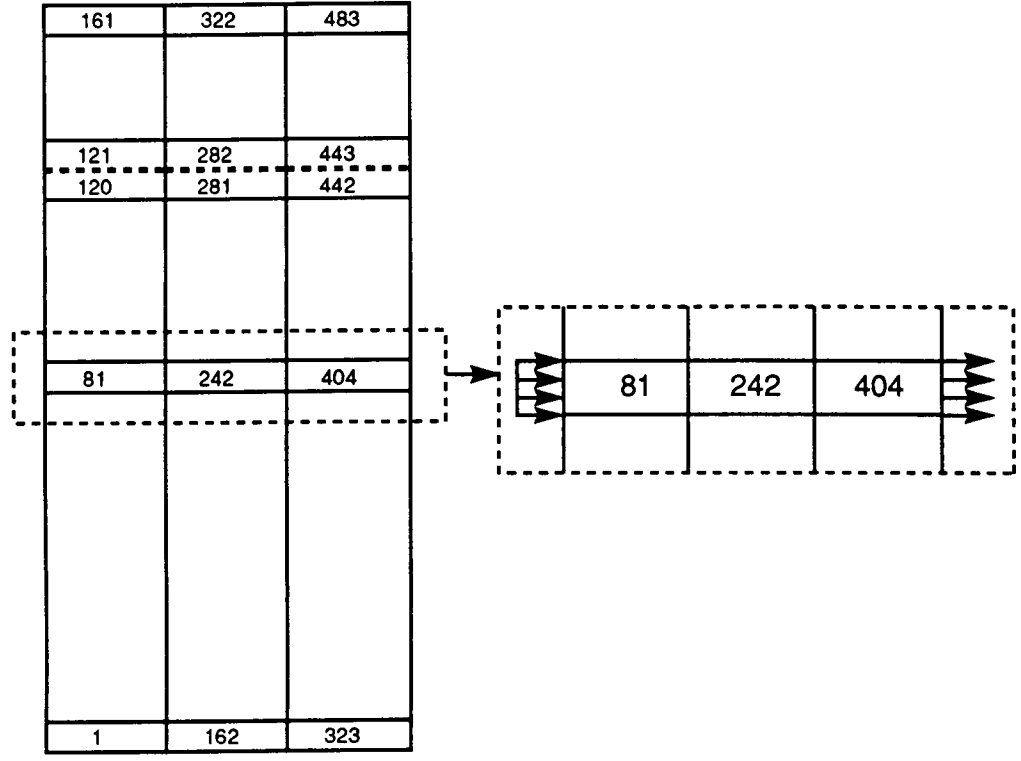


Figure 3.2 Problem Geometry for Analysis of Slip Induced by a Harmonic Shear Wave



(a)



(b)

Figure 3.3 Finite Element Discretizations for Element Distributions (a) and (b)

The geometric data for the model are as follows:

$$h = 16,100 \text{ m}$$

$$b = 100 \text{ m for discretization (a)}$$

$$= 300 \text{ m for discretization (b)}$$

$$s = 8050 \text{ m (center of element 81)}$$

$$a = 12,100 \text{ m}$$

### 3.4.2 Mechanical Properties of Continuous Media and Discontinuity

The rock material on opposite sides of the interface is taken to respond elastically to imposed load. Material type 6 is the relevant material specification in the input to the code, appropriate to materials exhibiting finite strain, elastic-plastic strain-hardening behavior. Elastic behavior is invoked by setting the yield stress parameters to zero.

With regard to the properties of the interface assigned in the analysis, it was noted previously that the shear force of the sliding interface in HONDO II is defined by Eq. 1.1. This involves the terms  $\mu_0$  and  $\mu_\infty$ , which are coefficients of friction for low and high sliding velocities respectively,  $\gamma$ , a decay constant characteristic of the transition between low and high sliding velocities, and  $v$ , the relative velocity between the opposing surfaces. In addition, two elastic constants,  $E_1$  and  $E_2$  (representing the rock mass on either side of the interface), are required for evaluation of restoring normal forces. Table 3.1 presents the values of these input parameters used for the current study.

Table 3.1

Mechanical Properties of the Elastic Media and Discontinuity

Intact Material Properties		Discontinuity Properties
Mass Density	2650 kg/m <sup>3</sup>	$\mu_0 = 0.0, 0.287, 0.7$
Young's Modulus	24.82 GPa	$\mu_\infty = 0$
Poisson's Ratio	0.42	$\gamma = 0$
Shear Wave Velocity	1942.5 m/sec	$E_1 = 24.82 \text{ GPa}$
		$E_2 = 24.82 \text{ GPa}$

### 3.4.3 Dynamic Loading

The harmonic pressure applied transversely to the central section of the model had the following characteristics.

maximum induced shear stress	1.0 MPa
frequency of incident wave	1 Hz
type of harmonic wave	sinusoidal
duration of incident wave	4 secs

In an initial analysis to examine code performance on a problem with a mode of response readily related to input conditions, the discontinuity was assigned properties intended to impose continuous elastic behavior of the block. However, it was found that HONDO II does not provide for perfect bonding of the sliding

interface. Subsequently, this problem was modeled without a joint. For problem discretization (a), a pressure of amplitude 1 MPa and frequency 1 Hz was applied on element 81 in the transverse direction. Four (4) Gauss points were chosen for the numerical integration, and the average of the stresses at these points was recorded as the stress history for a particular element. The shear stress was monitored at Points A, B, C, D, E and F, as shown in Figure 3.3. Points A, B, C, D and E are at distances 1000 m, 1900 m, 3700 m, 3900 m and 4000 m, respectively, from element 81. In the input of the applied load, a sinusoidal pressure history for a duration of 4 secs was discretized into 41 piece-wise linear increments. Pressures at the successive time intervals were input to the code.

In the subsequent analysis, a horizontal joint was introduced which transected the block. The joint was located a distance 4000 m above the point of load application. The shear wave was applied as a transversely applied sinusoidal load of magnitude 1 MPa, frequency 1 Hz and duration 4 secs. The shear stress histories were monitored at locations A through F (Fig. 3.3). All four boundaries are constrained to move only in the horizontal direction. The analysis was performed for three different values of the coefficient of friction,  $\mu_0$ .

### 3.5 RESULTS

For the preliminary elastic analysis, the time history of shear stress at points A through F is shown in Figure 3.4. The stress histories at all these points trace the sinusoidal input shear wave with peak amplitude of 1 MPa and are separated by time intervals consistent with their mutual separation and with the distance of these points from the source. This confirms that the model generates and transmits a plane shear wave to the far field and that spurious reflection of waves from the boundary did not distort the primary motion at the specified points during the elapsed time of the applied load.

Ideally, the performance of the code in analysis of the jointed block would be assessed by comparison of the acoustic coefficients for transmission, reflection and absorption at the interface, calculated from the numerical and analytical solutions. The comparison is conducted in terms of the dimensionless stress  $\tau_d$  of the incident wave, defined by

$$\tau_d = \omega \gamma \frac{U}{\tau_s} \quad (3.12)$$

where  $\omega$  = circular frequency of the incident wave,  
 $\gamma$  = mass density,  
 $U$  = displacement amplitude of the incident wave, and  
 $\tau_s$  = joint shear stress.

In developing the closed-form solution for the acoustic coefficients, Miller (1978) considered the shear resistance of the interface to be defined by a Coulomb friction law; i.e. for a cohesionless interface, the joint shear strength,  $\tau_s$ , is determined by the normal stress,  $\sigma_n$ , on the joint and the friction angle  $\phi$ , according to

$$\tau_s = \sigma_n \tan \phi \quad (3.13)$$

To achieve suitable states of stress on the joint to evaluate the effects of slip induced by the shear wave, it is necessary to control the normal stress  $\sigma_n$  independently of the shear stress. However, in HONDO II, it is not possible to apply two sets of boundary loads with independent time histories. The result is that it is not possible to apply a constant normal stress in the axial (vertical) direction while, at the same time, applying



NO SLIDING INTERFACE  
DISCRETIZATION A

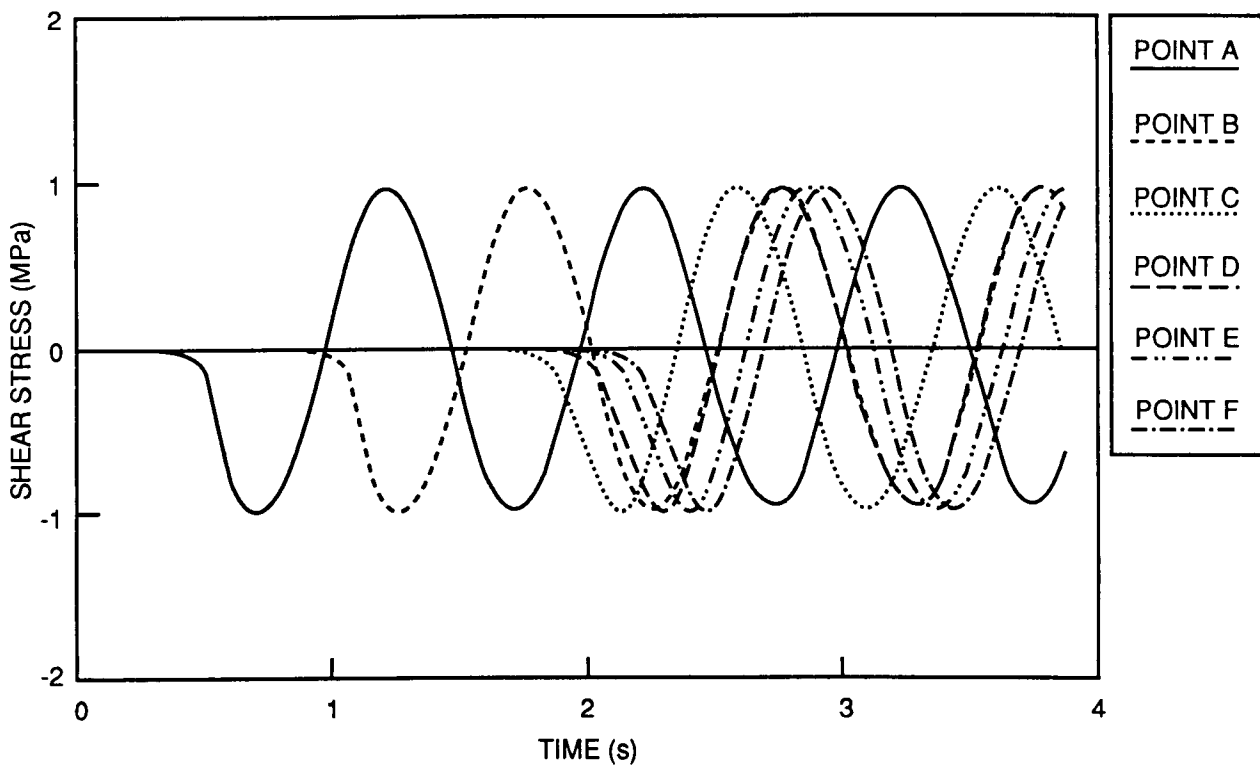


Figure 3.4 History of Shear Stress at Points A through F for Solid Block and Discretization Scheme (a)

time-dependent transverse (horizontal) load to the central part of the problem. As a result, the joint shear stress  $\tau_s$ , and the derived dimensionless stress  $\tau_d$ , cannot be varied independently of  $\sigma_n$ .

With these limitations, it was not possible to conduct the code assessment in terms of the acoustic coefficients. Instead, it was necessary to concentrate on characteristics of wave propagation for the case of zero applied normal load. The shear stress at Points A through F with friction coefficients  $\mu_0 = 0.0$  for the sliding interface are shown in Figures 3.5 and 3.6 for discretization schemes (a) and (b), respectively. From the history at Point F, it is clear that there is virtually no shear stress transmitted across the interface. Point A reaches steady state at the peak shear stress of 1 MPa. Point E is affected by the reflection due to slip at the interface. Points B, C and D, located at some distance from the interface, show amplification in shear stress. These points experience superposition of incoming waves from the source (i.e., point of load application), and the reflected wave from the joint. The behavior is consistent with a flexural mode of vibration. With the introduction of the joint and with no transverse restraint applied to it, the model behaves like a beam with a free end.

Figures 3.7 and 3.8 show the response at Points A through F for friction coefficients of 0.286 and 0.7 for discretization scheme (b). Comparing Figs. 3.6 through 3.8, response at the respective points appears similar for the different problem input parameters. Focusing attention on Point F in Figs 3.6 through 3.8, increasing the friction coefficient did not result in transmission of energy through the interface. This is because at the state of zero applied normal stress, the joint had no shear strength,  $\tau_s$ . The interface was incapable of supporting and transmitting the shear wave.

#### 4. CODE LIMITATIONS

In order to appreciate sources of difficulty in computational analysis of this problem with HONDO II, the following limitations in the code formulation may be noted.

- (1) The version of the code investigated here does not have provision for applying non-reflecting boundary conditions. The boundary of the model needs to be sufficiently remote to ensure that the transient response at the point of interest is not affected by the wave reflected from the boundary.
- (2) Input data for the joint properties are  $\mu_\infty$  (the friction coefficient for high sliding velocity),  $\mu_0$  (the friction coefficient for low sliding velocity), and  $\gamma$  (a decay constant). These properties are required to determine the joint shear strength through Eq. (1.1).

For most rock discontinuities, the friction coefficients at high and low sliding velocities and the decay constant are not known. In the current analysis,  $\mu_\infty$  and  $\gamma$  were assigned the value of zero, resulting in a linear (Coulomb) relation between shear stress and normal stress and zero joint cohesion. In that case, the friction coefficient at low sliding velocity determines the shear strength of the interface.

- (3) There is no option in HONDO II to generate a perfectly bonded or welded interface. Therefore, it was not possible to investigate the performance of the code in modeling perfect transmission across an interface of very high shear strength.
- (4) Evaluation of the dynamic performance of the discontinuity involves determination of transmission, reflection and absorption coefficients and comparison with closed-form solutions by Miller (1978).

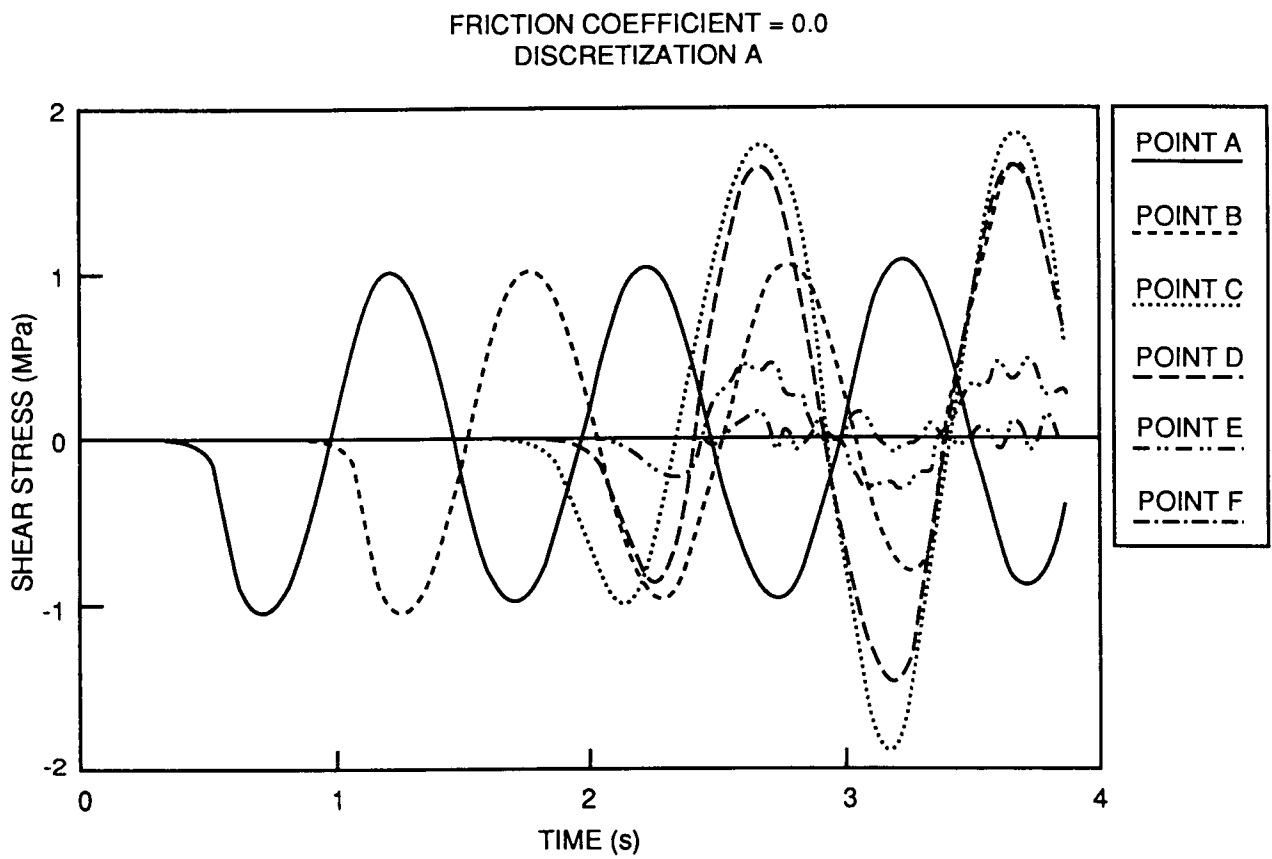


Figure 3.5 Shear Stress Histories for the Jointed Block at Points A through F, Coefficient of Friction = 0, Discretization Scheme (a)

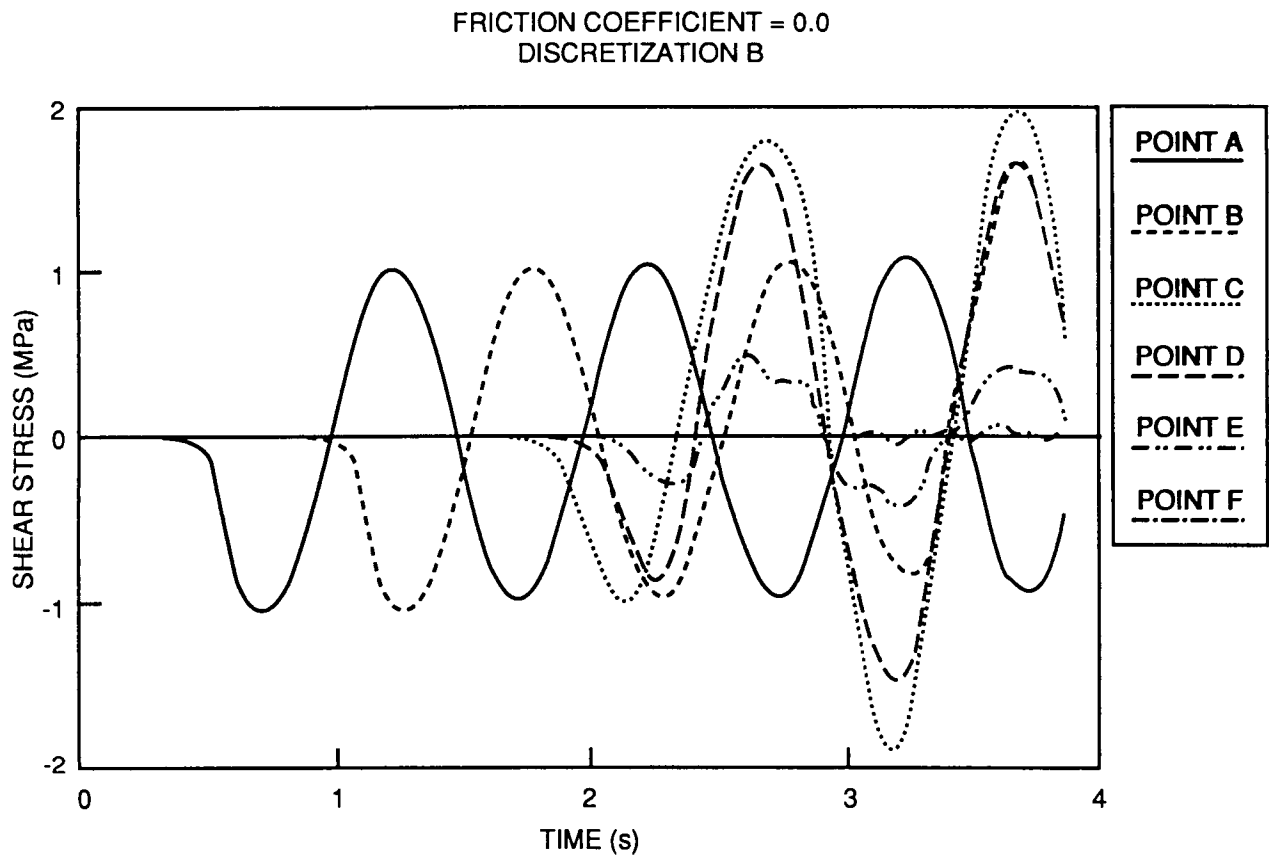


Figure 3.6 Shear Stress Histories at Points A through F, Coefficient of Friction = 0, Discretization Scheme (b)

FRICITION COEFFICIENT = 0.286  
DISCRETIZATION B

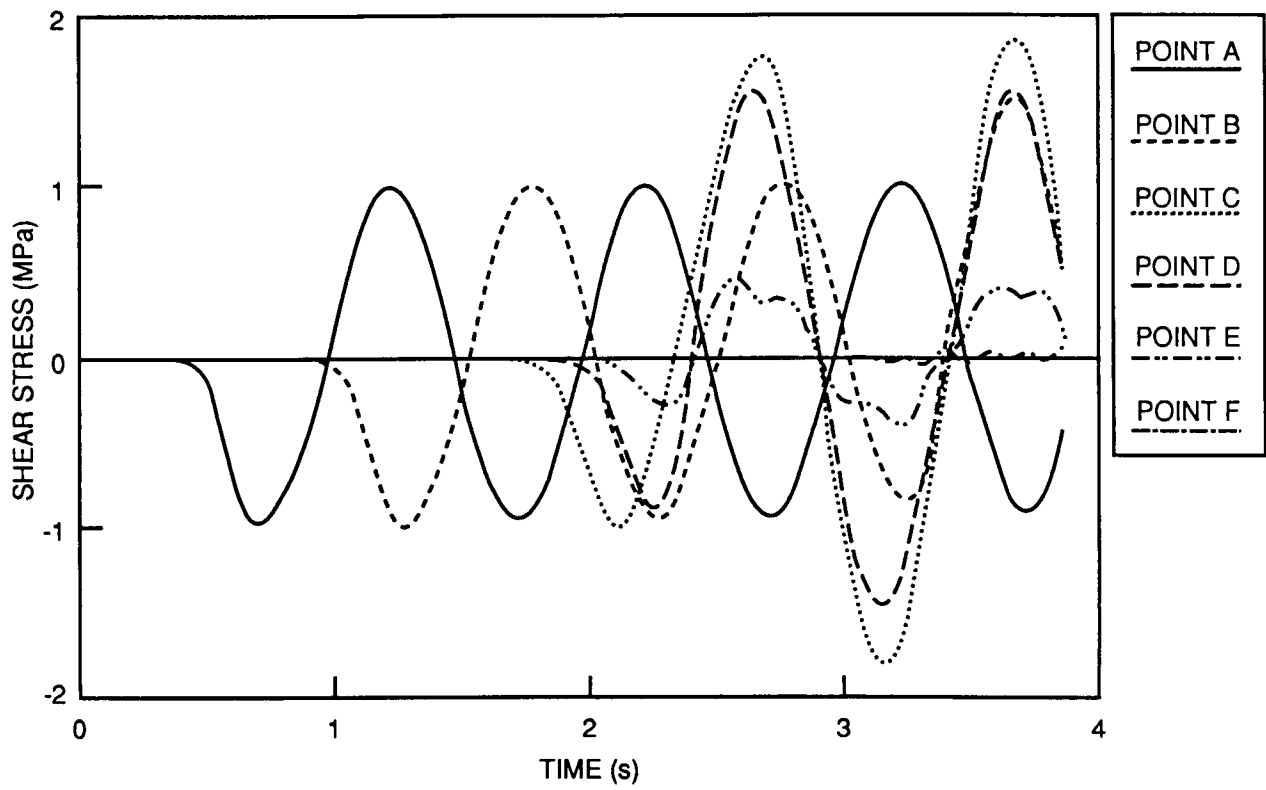


Figure 3.7 Shear Stress Histories at Points A through F, Coefficient of Friction = 0.286, Discretization Scheme (b)

FRICITION COEFFICIENT = 0.7  
DISCRETIZATION B

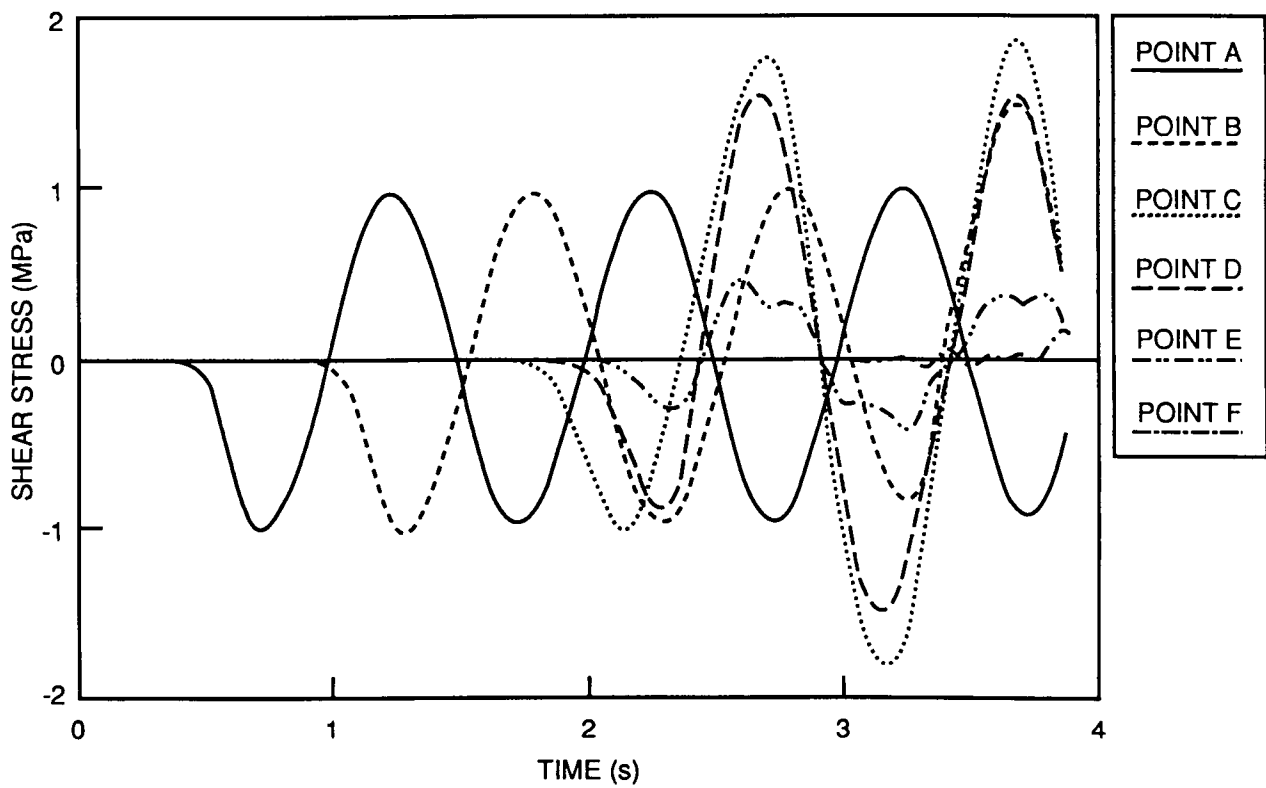


Figure 3.8 Shear Stress Histories at Points A through F, Coefficient of Friction = 0.7, Discretization Scheme (b)

In the analysis with HONDO II, it was not possible to apply independent stress components in a way which would permit evaluation of the various acoustic coefficients. It seems that a constant normal stress cannot be applied to the joint at the same time as a time-dependent shear wave is applied.

- (5) HONDO II has no bandwidth constraint because a stiffness matrix is not required, eliminating major storage requirements. However, the nodal numbering scheme in the mesh generation section of the code lacks flexibility. As a result, the generation of geometric data associated with the sliding interface becomes complicated and is best achieved manually.
- (6) The capacity to apply an external load to the boundary of a problem in terms of a normal traction or pressure only, severely restricts the code application and versatility. The nature of the permitted boundary loading reflects the application of the code intended originally, rather than a limitation in the formulation.

## 5. SUMMARY AND CONCLUSIONS

The intention in conducting the quasi-static and dynamic analyses of jointed blocks considered in this report was to determine if HONDO II could be applied in its current form to the static and dynamic analysis of jointed rock masses. A specific aim of the evaluation was to determine if the joint deformation model in HONDO II provides an adequate representation of the discontinuous deformation of jointed rock, resulting from slip or separation on planes of weakness embedded in an otherwise continuous solid. Both the benchmark problems considered in the study are concerned with joint slip, because this is regarded as a more acute problem in analysis than the mechanics of joint separation.

In the static deformation of a jointed elastic block subject to a load-unload cycle, the essential feature of the response is hysteresis in the load-displacement path resulting from joint slip and frictional locking at various stages of block deformation. The HONDO II analysis of a jointed block did not reproduce the expected hysteretic response. Because hysteresis in a load cycle is a highly discriminating test of the joint model, this result suggested the joint formulation in HONDO II is not sufficiently rigorous to express the mechanics of joint deformation. Because of some restrictions on the way in which boundary tractions may be applied in an analysis with HONDO II, it was not possible to conduct some simple test studies, such as analysis of a direct shear test, which would permit identification of the source of the problem. Further, it was considered that a detailed exploration of the code logic implementing the joint model was beyond the scope of the current project.

The evaluation of the capacity of HONDO II to simulate the dynamic response of a jointed medium was intended to be based on a comparison with the analytical solution for a shear wave propagating in a jointed block. A convenient way of doing this would be to compare the coefficients for energy transmission, reflection and absorption at the slipping interface, for the HONDO II and analytical solutions. The way in which boundary tractions can be specified in the code prevented making this comparison. The particular problem is that it is not possible to apply a static normal traction on one boundary and an independent, time-varying traction, either normal or shear, to another. This prevented application of a static normal stress to the joint, which is required to mobilize the joint shear strength and thus support wave propagation across it. Therefore, it was necessary to consider the performance of the code in simulating a jointed medium in qualitative terms, by examining the nature of the motion associated with shear wave interaction with a joint of zero shear strength. In this evaluation, the joint reflected the wave virtually completely.

It is concluded from the preceding discussion that, in its current formulation, HONDO II is not capable of simulating the mechanics of jointed rock in a way suitable for repository design and performance assessment. Some of its deficiencies in this respect are related to the application of static and dynamic boundary loads in the analysis. These reflect the original purpose of the code, which was for the analysis of

impact between finite bodies. However, the inadequacy of the interface formulation for simulation of joint static deformation implies this aspect of the code would need substantial improvement to permit its application in analysis of discontinuous deformation of jointed rock masses.

## 6. REFERENCES

- Banerjee, P. K., and S. Ahmad, 1985, "Advanced Three-Dimensional Dynamic Analysis by Boundary Element Methods," Advanced Topics in Boundary Element Analysis (T. A. Cruse et al., Eds.), Vol. 72, pp. 65-81. New York: ASME.
- Brady, B. H. G., M. L. Cramer and R. D. Hart, 1985, "Preliminary Analysis of a Loading Test on a Large Basalt Block" (Tech. Note), Int. J. Rock Mech. Min. Sci. & Geomech. Abstr., 22, 345-348.
- Cundall, P. A., 1988, "Formulation of a Three-Dimensional Distinct Element Model – Part I: A Scheme to Detect and Represent Contacts in a System Composed of Many Polyhedral Blocks," Int. J. Rock Mech., Min. Sci. & Geomech. Abstr., 25, 107-116.
- Hsiung, S. M., D. D. Kana, B. H. G. Brady and A. H. Chowdhury, 1989, Project Plan for Seismic Rock Mechanics Project. Center for Nuclear Waste Regulatory Analyses, Nuclear Regulatory Commission, Contract NRC-02-88-005.
- Jaeger, J. C., and N. G. W. Cook, 1976, Fundamentals of Rock Mechanics, 2nd Ed., pp. 329-333. London: Chapman and Hall.
- Kana, D. D., B. H. G. Brady, B. W. Vanzant and P. K. Nair, 1989, Critical Assessment of Seismic and Geomechanics Literature Related to a High-Level Nuclear Waste Underground Repository. Center for Nuclear Waste Regulatory Analyses, Report 89-001.
- Key, S. W., 1986, "A Data Structure for Three-Dimensional Sliding Interfaces," Int. Conf. on Computational Mechanics (Tokyo, Japan).
- Key, S. W., Z. E. Beisinger and R. D. Krieg, 1978, "HONDO II – A Finite Element Computer Program for the Large Deformation Dynamics Response of Axisymmetric Solids," Sandia National Laboratories, SAND78-0422.
- Kolsky, H., 1963, Stress Waves in Solids. New York: Dover Publications.
- Miller, R. K., 1978, "The Effects of Boundary Friction on the Propagation of Elastic Waves," Bull. Seis. Soc., 68, 987-998.
- Olsson, W. A., 1982, "Experiments on a Slipping Crack," Geophys. Res. Letters, 9(8), pp. 797-800.
- Walsh, J. B., 1965, "The Effect of Cracks on the Compressibility of Rock," J. Geophys. Res., 70, 381-389.
- Williams, J. R., G. Hocking and G. G. W. Mustoe, 1985, "The Theoretical Basis of the Discrete Element Method," Proceedings of the NUMETA '85 Conference, pp. 897-906.
- Zienkiewicz, O. C., 1977, The Finite Element Method, 3rd Ed., London: McGraw-Hill.



**APPENDIX 1 – HONDO II INPUT DATA FILES**

INPUT DATA FILES

HONDO: elastic matrix with 45 deg slide line - friction coeff 0.287  
1 328 288 12 4 3 1.0e6 1 0 1 4 1 500  
0.  
0.0 .2 .05 0.0 .2 .005 500.0  
313 315 317 319 321 323 325  
7 282  
1 6 2850.0  
Generic rock properties  
85.11e9  
0.21

1	2.	1.000	.000
2	2.	1.083	.000
3	2.	1.167	.000
4	2.	1.250	.000
5	2.	1.309	.000
6	2.	1.417	.000
7	2.	1.500	.000
8	2.	1.583	.000
9	2.	1.691	.000
10	2.	1.750	.000
11	2.	1.833	.000
12	2.	1.917	.000
13	2.	2.000	.000
14		1.000	.042
15		1.083	.049
16		1.167	.056

nodal point coordinates discontinued here,  
but are present in the original input file

322		1.750	2.000		
323		1.833	2.000		
324		1.917	2.000		
325		2.000	2.000		
326		1.417	.917		
327		1.500	1.000		
328		1.583	1.083		
1	1	2	15	14	1
2	2	3	16	15	1
3	3	4	17	16	1
4	4	5	18	17	1
5	5	6	19	18	1
6	6	7	20	19	1
7	7	8	21	20	1

element connection array discontinued here,  
but are present in the original input file

```

281 304 305 318 317 1
282 305 306 319 318 1
283 306 307 320 319 1
284 307 308 321 320 1
285 308 309 322 321 1
286 309 310 323 322 1
287 310 311 324 323 1
288 311 312 325 324 1
313 314 1.e+0 1.e+0 0.
314 315 1.e+0 1.e+0 0.
315 316 1.e+0 1.e+0 0.
316 317 1.e+0 1.e+0 0.
317 318 1.e+0 1.e+0 0.
318 319 1.e+0 1.e+0 0.
319 320 1.e+0 1.e+0 0.
320 321 1.e+0 1.e+0 0.
321 322 1.e+0 1.e+0 0.
322 323 1.e+0 1.e+0 0.
323 324 1.e+0 1.e+0 0.
324 325 1.e+0 1.e+0 0.
0. .001
1.0e-1 8.5e+6
1.5e-1 5.0e+6
2.0e-1 .001
1
328
1 3 3
85.11e9 85.11e9 .287 0. 0.
162 163 164
326 327 328
end

```

MILLER PROBLEM PROPAGATION OF SHEAR WAVE WITHOUT SLIPPING INTERFACE

```

1 324 161 2 41 3 1.0e5 1 0 0 4 1 0 0
0.0 .4e1 .1e-2 0.0 0.000 0.000 5
241
90 100 115 118 120 121
1 6 2650.0
property of rock mass
24.83e9
0.42

```

```

1 2 1.000 1.000
323 2 1.000 16101.000 2
2 2 101.000 1.000
324 2 101.000 16101.000 2
1 1 2 4 3 1
2 3 4 6 5 1
3 5 6 8 7 1
4 7 8 10 9 1
5 9 10 12 11 1

```

element connection arrays discontinued here, but are present in the original input file.

```

155 309 310 312 311 1
156 311 312 314 313 1
157 313 314 316 315 1
158 315 316 318 317 1
159 317 318 320 319 1
160 319 320 322 321 1
161 321 322 324 323 1
163 161 1. 1. .000
164 162 -1. -1. .000
.000 .1e-3
.1 .587e6
.2 0.95e6
.3 .951e6
.4 .588e6
.5 .0016e6
.6 -.586e6
.7 -.950e6
.8 -.951e6
.9 -.590e6
1.0 -.0032e6
1.1 .585e6
1.2 .949e6

```

1.3 .952e6  
1.4 .591e6  
1.5 .0047e6  
1.6 -.583e6  
1.7 -.949e6  
1.8 -.953e6  
1.9 -.592e6  
2.0 -.0064e6  
2.1 0.5823e6  
2.2 0.9488e6  
2.3 0.9533e6  
2.4 0.5939e6  
2.5 0.7960e3  
2.6 -.581e6  
2.7 -.9483e6  
2.8 -.9537e6  
2.9 -.5950e6  
3.0 -.9550e3  
3.1 .5797e6  
3.2 .9478e6  
3.3 .9542e6  
3.4 .5965e6  
3.5 .0110e6  
3.6 -.5784e6  
3.7 -.9473e6  
3.8 -.9547e6  
3.9 -.5977e6  
4.0 -.0127e6

1 0. .00  
324 0. .00 1  
END

INPUT DATA FILE FOR DISCRETIZATION SCHEME (a)

MILLER PROBLEM; SLIPPING JOINT FRIC. COEFF. = 0.0.

```

1 326 161 2 41 3 1.0e5 1 0 1 4 1 0 0
0.0 .4e1 .1e-2 0.0 0.000 0.000 5
241 243
90 100 115 118 120 121
1 6 2650.0
property of rock mass
24.83e9
0.42

```

```

1 2 1.000 1.000
239 2 1.000 11901.000 2
2 2 101.000 1.000
240 2 101.000 11901.000 2
241 0 1.000 12001.000
242 0 101.000 12001.00
243 0 1.000 12001.000
244 0 101.000 12001.00
245 2 1.000 12101.00
325 2 1.000 16101.000 2
246 2 101.000 12101.000
326 2 101.000 16101.000 2
1 1 2 4 3 1
2 3 4 6 5 1
3 5 6 8 7 1
4 7 8 10 9 1
5 9 10 12 11 1
6 11 12 14 13 1
7 13 14 16 15 1
8 15 16 18 17 1
9 17 18 20 19 1
10 19 20 22 21 1
11 21 22 24 23 1

```

element connection arrays discontinued here, but are present in the original input file.

153	307	308	310	309	1		
154	309	310	312	311	1		
155	311	312	314	313	1		
156	313	314	316	315	1		
157	315	316	318	317	1		
158	317	318	320	319	1		
159	319	320	322	321	1		
160	321	322	324	323	1		
161	323	324	326	325	1		
163	161		1.		1.		.000
164	162		-1.		-1.		.000
	.000		.1e-3				
	.1		.587e6				
	.2		0.95e6				
	.3		.951e6				
	.4		.588e6				
	.5		.0016e6				
	.6		-.586e6				
	.7		-.950e6				
	.8		-.951e6				
	.9		-.590e6				
	1.0		-.0032e6				
	1.1		.585e6				
	1.2		.949e6				
	1.3		.952e6				
	1.4		.591e6				
	1.5		.0047e6				
	1.6		-.583e6				
	1.7		-.949e6				
	1.8		-.953e6				
	1.9		-.592e6				
	2.0		-.0064e6				
	2.1		0.5823e6				
	2.2		0.9488e6				
	2.3		0.9533e6				
	2.4		0.5939e6				
	2.5		0.7960e3				
	2.6		-.581e6				
	2.7		-.9483e6				
	2.8		-.9537e6				
	2.9		-.5950e6				
	3.0		-.9550e3				
	3.1		.5797e6				
	3.2		.9478e6				
	3.3		.9542e6				
	3.4		.5965e6				
	3.5		.0110e6				
	3.6		-.5784e6				

```
3.7 -.9473e6
3.8 -.9547e6
3.9 -.5977e6
4.0 -.0127e6
1      0.      .00
326    0.      .00    1
1      2      2
24.82e9 24.82e9 0.00    0      0
241 242
243 244
END
```



INPUT DATA FILE DISCRETIZATION SCHEME (b)

MILLER PROBLEM; SLIPPING JOINT FRIC. COEFF. = 0.0  
 1 652 483 2 41 3 1.0e5 1 0 1 4 1 0 0  
 0.0 .4e1 .1e-2 0.0 0.000 0.000 5  
 283 650  
 251 261 276 279 281 282  
 1 6 2650.0  
 property of rock mass  
 24.83e9  
 0.42

1	2	1.000	1.000		
120	2	1.000	11901.000	1	
121	0	1.000	12001.000		
122	2	1.000	12101.000		
162	2	1.000	16101.000	1	
163	2	101.000	1.000		
282	2	101.000	11901.000		
283	0	101.000	12001.000		
284	2	101.000	12101.000		
324	2	101.000	16101.000	1	
325	2	201.000	1.000		
444	2	201.000	11901.000		
445	0	201.000	12001.000		
446	2	201.000	12101.000		
486	2	201.000	16101.000	1	
487	2	301.000	1.000		
606	2	301.000	11901.000		
607	0	301.000	12001.000		
608	2	301.000	12101.000		
648	2	301.000	16101.000	1	
649	0	1.000	12001.000		
650	0	101.000	12001.000		
651	0	201.000	12001.000		
652	0	301.000	12001.000		
1	1	163	164	2	1
2	2	164	165	3	1
3	3	165	166	4	1
4	4	166	167	5	1
5	5	167	168	6	1
6	6	168	169	7	1
7	7	169	170	8	1
8	8	170	171	9	1
9	9	171	172	10	1
10	10	172	173	11	1

element connection arrays discontinued here, but are present in the original input file.

476	478	640	641	479	1		
477	479	641	642	480	1		
478	480	642	643	481	1		
479	481	643	644	482	1		
480	482	644	645	483	1		
481	483	645	646	484	1		
482	484	646	647	485	1		
483	485	647	648	486	1		
82	81		3.		3.		.000
568	567		-3.		-3.		.000
	.000		.1e-3				
	.1		.587e6				
	.2		0.95e6				
	.3		.951e6				
	.4		.588e6				
	.5		.0016e6				
	.6		-.586e6				
	.7		-.950e6				
	.8		-.951e6				
	.9		-.590e6				
	1.0		-.0032e6				
	1.1		.585e6				
	1.2		.949e6				
	1.3		.952e6				
	1.4		.591e6				
	1.5		.0047e6				
	1.6		-.583e6				
	1.7		-.949e6				
	1.8		-.953e6				
	1.9		-.592e6				
	2.0		-.0064e6				
	2.1		0.5823e6				
	2.2		0.9488e6				
	2.3		0.9533e6				
	2.4		0.5939e6				
	2.5		0.7960e3				
	2.6		-.581e6				
	2.7		-.9483e6				
	2.8		-.9537e6				
	2.9		-.5950e6				
	3.0		-.9550e3				
	3.1		.5797e6				
	3.2		.9478e6				
	3.3		.9542e6				
	3.4		.5965e6				

	3.5	.0110e6			
	3.6	-.5784e6			
	3.7	-.9473e6			
	3.8	-.9547e6			
	3.9	-.5977e6			
	4.0	-.0127e6			
1		0.	.00		
652		0.	.00	1	
1	4	4			
24.82e9	24.82e9	0.00		0	0
649	650	651	652		
121	283	445	607		

END